

Assessment of the Water Vapor Permeability: Effect of the total pressure

Thierry Duforestel^{a,c,*}, Imane Oubrahim^{a,b,c}, Rafik Belarbi^{b,c}, Hanaa El Hardouz^a, Mathilde Colmet Daâge^{a,c}

^aEDF R&D, TREE, EDF Lab Les Renardières, 77818 Moret-sur-Loing, France

^bLaSIE, UMR 7356, CNRS, La Rochelle Université, Avenue Michel Crépeau, 17042 La Rochelle Cedex 1, France

^c4ev Lab, CNRS, Université de La Rochelle, Electricité de France EDF, Avenue Michel Crépeau, 17042 La Rochelle Cedex 1, France

Abstract

This paper shows that the theory describing gas diffusion with no consideration of the total gas pressure leads to an underestimation of the water vapor diffusive permeability. This experimental method, called cup method, can be considered as one of the most popular tests in the domain of heat and mass transfer for building applications. Thus, it is likely that the water vapor permeability defined for most current building materials is underestimated. Thanks to the approach proposed in this paper, provided that there is an advective gas permeability, it is possible to know whether a given water vapor permeability has been underestimated or not. However, it is not possible to estimate the magnitude of this measurement error. In the last part, a new experimental procedure is proposed, integrating a total gas pressure measurement on both sides of the sample. This modified test method makes it possible to simultaneously determine the advective gas permeability and the diffusive vapor transfer coefficient.

Keywords: Water vapor permeability, hygrothermal modeling, advection, total gas pressure, cup test method

*Corresponding author

Email addresses: imane.oubrahim@edf.fr (Imane Oubrahim),
rafik.belarbi@univ-lr.fr (Rafik Belarbi), hanaa.el-hardouz@edf.fr (Hanaa El Hardouz),
mathilde.colmet-daage@edf.fr (Mathilde Colmet Daâge)

URL: thierry.duforestel@edf.fr (Thierry Duforestel)

1. Highlights

- Modeling of coupled heat and moisture transfer within porous materials;
- Protocol of water vapor permeability measurement using the cup test method;
- 5 • Consideration of advection in water vapor permeability evaluation;
- New experimental protocol to determine two transfer properties: water vapor permeability and relative gas permeability using a modified cup test method;

2. Introduction

10 Since the introduction of the GLASER method in current building physics practices [1], many more sophisticated models have been developed to study the evolution of heat, air, and moisture in porous materials used in building components ([2, 3, 4, 5], etc.). Some of these coupled models have led to the development of simulation software tools (e.g., WUFI ([6] and [7]), DELPHIN
15 [8], TRNSYS [9], Energy Plus [10]). Nevertheless, it appears that most of these tools include a simplified expression of gas diffusion, very close to the GLASER expression, for which the total gas pressure has no impact on diffusion. This approximation can be accepted for materials with high gas permeability. But for materials with low gas permeability (e.g., concrete), this diffusion expression
20 fails to represent the actual behavior of gas in some specific configurations. It is particularly true when the gas transfer phenomenon by both advection and diffusion compete, like in some drying processes ([11, 12, 13]).

The total gas pressure impact is rarely included in the mass transfer occur-
25 ring in building envelope components. This is probably since the reference model in this domain (the GLASER model [1]) did not consider the total gas pressure.

Nevertheless, it seems essential to keep in mind its potential consequences in some configurations. As far as the physics of gas transfer is concerned, there is no reason why the total gas pressure should be uniform and constant over
30 time. Total gas pressure evolutions are part of the overall gas behavior in porous media and must be considered with the rest of the partial pressures.

One of the configurations where the total gas pressure is most often considered uniform is the cup test method. It's a normalized test [14] used to measure the water vapor permeability. We think that, in this configuration, neglecting the
35 total gas pressure could lead to an underestimation of the measured coefficient. There are only a few studies on the impact of this assumption on measurements. Nevertheless, some experimental attempts more than 20 years ago [15] have partly explored this issue, especially by carrying out cup tests in low gas pressure conditions.

40 In this paper, we propose to study the impact of total gas pressure in a well-known configuration: the cup test method. First, we will analyze this test physically, using complete expressions of flow formulas. Then, numerically, using the SYRTHES tool for coupled heat and mass transfer. Finally, we will propose a new test procedure to measure the water vapor diffusion coefficient,
45 considering the total gas pressure. In this paper, we are interested in analyzing the cup test method at a macroscopic scale, for water vapor transport in dry materials. Certainly, other interpretation issues are arising when the cup test method is operated with wet materials. It has been observed that the increase of the average RH leads to an apparent increase of measured water vapor permeability [16]. This specific and very important point will not be considered in
50 this paper.

3. Material and methods

3.1. Hygrothermal modeling

Originally, SYRTHES (SYstème de Résolution de la THERmique Solide) was
55 developed at EDF R&D for the pure thermal calculation of complex finite ele-

ment structures in $2D$ and $3D$. Its vocation was to couple with existing fluid thermal tools to integrate their results as boundary conditions of the solid problem and vice versa.

60 In its basic version, SYRTHES had a large variety of boundary conditions, including the possibility to compute the radiative exchange between external surfaces taking into account mask and screen effects. The formal similarity between the heat equation and the mass transfer equations (they are based on a diffusive formalism.) and the richness of the boundary conditions encouraged
65 us to exploit this platform to integrate the coupled resolution of the heat, water mass, and dry air mass conservation equations. We now integrate these features into the current version of SYRTHES [17].

The physical model used to model coupled heat and moisture transfer in
70 SYRTHES is based on three conservation equations [18]:

- Water mass conservation equation;
- Dry air mass conservation equation;
- Heat conservation equation.

For each of them, the structure is strictly identical. The first member represents the accumulation of the transferring entity (mass of water, mass of dry
75 air or heat) per unit of time and per unit volume of the porous medium. The second member represents the difference between the incoming flow and the outgoing flow at the border of the elementary volume. In its differential form, this balance is expressed as the divergence in the density of flow of the transferring
80 entity. The hypothesis included in these equations are:

- The equations of state of the fluids included in the porous medium are assumed to be conserved. This hypothesis implies that the interactions

85 between the fluids and the solid are assumed to be concentrated in the
moisture content;

- The gas phase is assumed to consist of an ideal mixture of two ideal
gases, the water vapor, and dry air. This assumption implies that each
component of the mixture respects the ideal gas law ($p_i = \rho_i \times r_i \times T$ for
 $i = as$ and $i = v$) and that the sum of partial pressures is equal to the
90 total pressure of the gas mixture;
- Everywhere in the porous medium and at every moment, all the phases
are in equilibrium. This imposes that at any point of the medium, the
temperatures of all phases are permanently equal. It also means that the
two phases of water which coexist in the medium are in thermodynamic
95 equilibrium;
- Finally, to avoid an unnecessary complication when we focus on the de-
scription of transfer phenomena, we will consider that the skeleton is non-
deformable and chemically inert with respect to its environment. The
main consequence of this assumption is that the dry porosity ϵ_0 remains
100 constant.

To summarize, our physical model is represented by the following equations:

Water mass conservation equation:

$$\begin{aligned} (\beta_p - \frac{\varepsilon p_v}{r_v T^2}) \frac{dT}{dt} + (\alpha_T + \frac{\varepsilon}{r_v T}) \frac{dp_v}{dt} = \vec{\nabla} \cdot (K_l \rho_l (r_v \ln(\frac{p_v}{p_{sat}(T)})) - \frac{L(T)}{T}) \vec{\nabla} T \\ + (\frac{\pi_v^*}{p_t} + K_l \frac{\rho_l r_v T}{p_v}) \vec{\nabla} p_v + (\omega_{mv} K_t - \frac{p_v \pi_v^*}{p_t^2}) \vec{\nabla} p_t \end{aligned} \quad (1)$$

Dry air mass conservation equation:

$$\begin{aligned} - \frac{(p_t - p_v)}{r_{as} T} (\frac{\beta_p}{\rho_l} + \frac{\varepsilon}{T}) \frac{dT}{dt} - \frac{1}{r_{as} T} (\frac{\alpha_t (p_t - p_v)}{\rho_l} + \varepsilon) \frac{dp_v}{dt} + \frac{\varepsilon}{r_{as} T} \frac{dp_t}{dt} \\ = \vec{\nabla} \cdot ((-\frac{\pi_v^* M_{as}}{p_t M_v}) \vec{\nabla} p_v + (\rho_{as} \frac{K k_{rg}}{\eta_t} + \frac{\pi_v^* p_v M_{as}}{p_t^2 M_v}) \vec{\nabla} p_t) \end{aligned} \quad (2)$$

Heat conservation equation:

$$\begin{aligned}
& (\rho_s C_s + \tau_v C_l - \tau_v h_p + \varepsilon \rho_v (C_l + \frac{dL(T)}{dT})) + \varepsilon \rho_{as} C_{pas} - (L(T) + h^m) (\frac{\beta_p p_v}{\rho_l r_v T} \\
& + \frac{\varepsilon p_v}{r_v T^2}) + \frac{p_t \beta_p}{\rho_l} \frac{dT}{dt} + (-\tau_v h_T + (L(T) + h^m) (-\frac{p_v \alpha_T}{\rho_l r_v T} + \frac{\varepsilon}{r_v T}) + \frac{p_t \alpha_T}{\rho_l}) \frac{dp_v}{dt} \\
& - \varepsilon \frac{dp_t}{dt} = \vec{\nabla} \cdot (\lambda^* \vec{\nabla} T + (L(T) + h^m) (\frac{\pi_v^*}{p_t}) \vec{\nabla} p_v + (L(T) + h^m) (\omega_{mv} K_t - \frac{\pi_v^* p_v}{p_t^2}) \vec{\nabla} p_t)
\end{aligned} \tag{3}$$

105 **Definition of boundary conditions:**

Mass and heat exchange between the environment and the porous medium are also coupled in SYRTHES:

Description of moisture flow:

$$\vec{g}_v = \bar{h}_v (\frac{p_{vext}}{p_{ttext}} - \frac{p_{vsurf}}{p_{tsurf}}) + \omega_{mv} \bar{h}_t (p_{ttext} - p_{tsurf}) \tag{4}$$

Description of dry air flow:

$$\vec{g}_{as} = \frac{M_{as}}{M_v} \bar{h}_v (\frac{p_{vsurf}}{p_{tsurf}} - \frac{p_{vext}}{p_{ttext}}) + (1 - \omega_{mv}) \bar{h}_t (p_{ttext} - p_{tsurf}) \tag{5}$$

Description of heat flow:

$$\vec{g}_c = \bar{h}_c (T_{ext} - T_{surf}) + L(T) \vec{g}_v \tag{6}$$

EDF R&D uses the SYRTHES tool in many projects, Ph.D. Thesis, and internships. Through these utilizations, this tool showed great accuracy with
110 theoretical expectations and experimental results.

HYGRO-BAT [19] is a project where EDF R&D and four other partners validated and compared their numerical tools for heat and moisture transfer simulation (including SYRTHES). Three partners involved in this project tested

115 four panels configuration (simple wall of wood fiber, double panels of wood fiber,
double panels of wood fiber with exterior coating, and double panels of wood
fiber with external coating and a layer of OSB in the internal part), with three
types of boundary conditions (isotherm, non-isotherm, and dynamic) to measure
temperature and moisture evolution through the tested panels. Then, they used
120 them to validate the four simulation tools. The comparison between the various
tools and the experimental results showed satisfactory results and opened the
door for further hypotheses to be investigated [20].

3.2. *The cup test method and its usual interpretation*

The cup test method is probably the best known experimental method in the
field of hygrothermal approaches for construction ([21], [22], [23]) . It is imple-
mented by almost all institutions involved in this domain and was standardized
almost 20 years ago at the level of the European Union and the whole world (NF
EN ISO 12572 October 2001 [14]). In principle, the cup test method is used to
measure the water vapor permeability π that appears in the GLASER model.
Indeed, according to this model, the mass flow rate of water vapor through a
porous material is written as:

$$g_v = -\pi \nabla p_v \quad (7)$$

The principle of this method is then straightforward. It consists of sealing a
125 sample of the material tested in the neck of a cup, where we maintain a con-
stant relative humidity using a saturated salt solution. This assembly is then
placed in a climatic room in which a different relative humidity is maintained
at a constant temperature. As it is not thermally insulated, the assembly is
supposed to be kept at climatic room temperature.

130

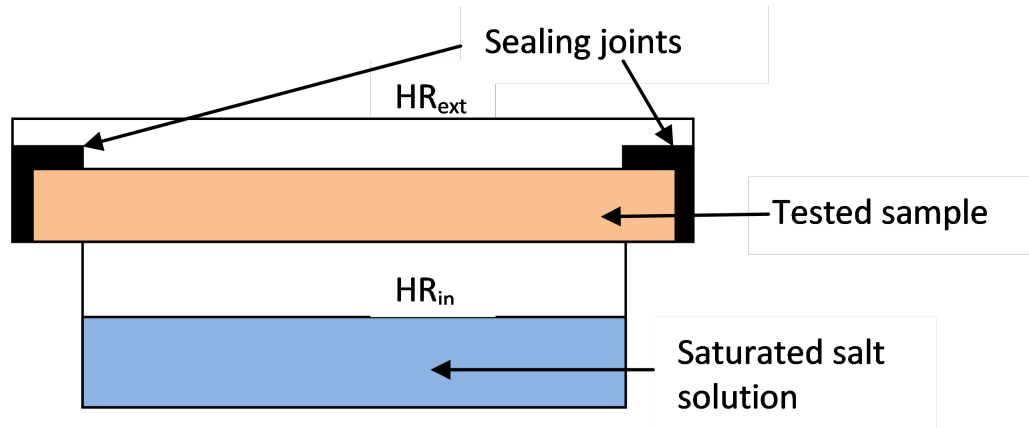


Figure 1: Typical assembly used for the cup test method

A differential in partial pressure of water vapor is thus created, then a mass vapor flow occurs from the higher vapor pressure to the lower one. The assembly is then regularly weighed. The saturated salt solution in the cup is used either as a source or as a sink. Thus the water vapor flowing through the sample can only condense in the salt or evaporate from it. The change in mass over time thus reveals the mass flow rate through the sample. When the steady-state is reached, this mass flow rate remains constant. And its value can be used to estimate the water vapor permeability of the material tested by the following equation:

$$\pi = \frac{g_v e}{\Delta p_v} \quad (8)$$

Special care should be taken for most water vapor permeable materials, as the external boundary conditions and the internal air layer can introduce significant resistances to water vapor transfer. These resistances must be accounted for in the final permeability estimation [24]. For this reason, it is recommended to maintain high air velocities in the climatic room and to estimate the internal air layer thickness to ultimately determine the permeability value of the sample itself and not the apparent permeability of the tested assembly. At this level of our presentation, it is interesting to keep in mind that neglecting this correction

will lead to an under-evaluated permeability.

140 *3.3. What about this interpretation of the cup test method?*

In its complete description, the water vapor mass flow rate through a porous media can be represented as the sum of two parallel flows:

A diffusive mass flow rate due to a gradient of the molecular ratio in the gas mixture:

$$\vec{g}_{v,diff} = -\pi_v \vec{\nabla} \frac{p_v}{p_t} \quad (9)$$

An advective mass flow rate due to a gradient of total pressure:

$$\vec{g}_{v,adv} = -\omega_{mv} K_t \vec{\nabla} p_t \quad (10)$$

Both these elementary phenomena can then be combined in a global vapor flow rate expression which can be developed as:

$$\vec{g}_v = -\frac{\pi_v^*}{p_t} \vec{\nabla} p_v - \left(\omega_{mv} K_t - \frac{p_v \pi_v^*}{p_t^2} \right) \vec{\nabla} p_t \quad (11)$$

145 It then appears that the standard cup test method interpretation can be accepted only if the second part of the flow expression can be considered as negligible. In such conditions, the mass flow rate expression is:

$$\vec{g}_v = -\frac{\pi_v^*}{p_t} \vec{\nabla} p_v \quad (12)$$

And the water vapor permeability can be estimated by:

$$\pi = \frac{\pi_v^*}{p_t} \quad (13)$$

Nevertheless, there is no apparent physical reason explaining that the term $\omega_{mv} K_t - \frac{p_v \pi_v^*}{p_t^2}$ should always have a very weak value. The only hypothesis that could justify this standard interpretation of the cup test method is that the total gas pressure gradient is always very weak, i.e., that the total gas pressure is always almost uniform. 150 The following part will show that this hypothesis cannot be admitted.

3.4. Total gas pressure distribution in the cup test configuration

155 First, we can give a purely phenomenological explanation. The cup test method is based on the use of a source and a sink of water vapor. This source and sink ensure the constant difference of partial vapor pressure between the two sides of the sample, leading to the existence of a steady state for the determination of water vapor permeability.

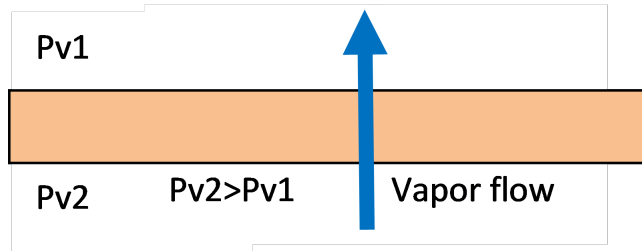


Figure 2: vapor flow across the sample

160 Should the total gas pressure be uniform, given that the gas is considered as an ideal mixture of perfect gases, a constant difference of dry air partial pressure would exist between both sides of the sample, thus a permanent diffusive mass flow of dry air would appear across the sample?

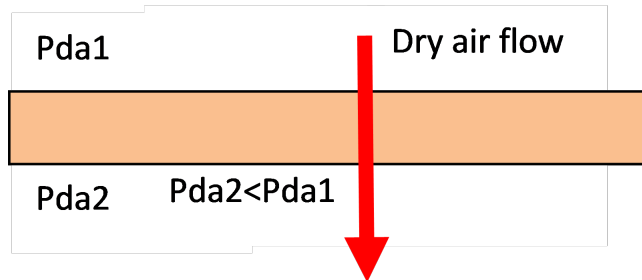


Figure 3: Dry air flow across the sample

165 However, this is impossible as there is neither source nor a sink of dry air in the cup. Where would this permanent dry air mass flow go or come from? As a result, a difference in total gas pressure between the two sides of the

sample should exist. This total gas pressure difference is necessary to create an advective mass flow rate of dry air that compensates for the diffusive dry air mass flow rate in a steady state.

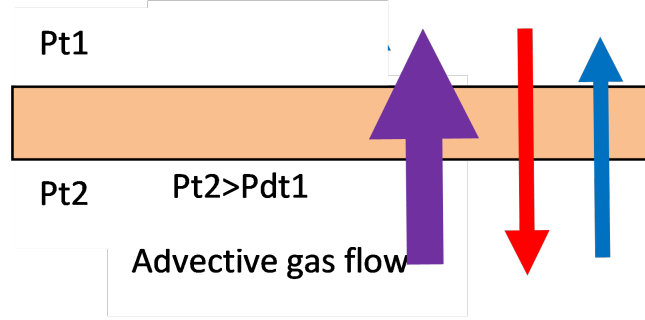


Figure 4: Advective gas flow for compensating the diffusive dry air flow

170 The cup test method is an experimental configuration for which the steady mass flow rate of dry air can only be zero.

The expressions of dry air and water vapor mass flow rates can be written as the sum of their diffusive and advective contributions:

$$\vec{g}_{da} = -\pi_{da}^* \vec{\nabla} \frac{p_{da}}{p_t} - \frac{\rho_{da}}{\rho_t} K_t \vec{\nabla} p_t \quad (14)$$

$$\vec{g}_v = -\pi_v^* \vec{\nabla} \frac{p_v}{p_t} - \frac{\rho_v}{\rho_t} K_t \vec{\nabla} p_t \quad (15)$$

The gas phase being considered as an ideal mix of two perfect gases (dry air and water vapor), the following equation can be derived:

$$p_{da} = p_t - p_v \quad (16)$$

leading to:

$$\vec{\nabla} \frac{p_{da}}{p_t} = -\vec{\nabla} \frac{p_v}{p_t} \quad (17)$$

In a configuration for which the total gas pressure is uniform, but dry air and vapor partial pressures are not uniform, the global mass flow rate must be

zero although there is an internal reorganization of the gas composition through a vapor and dry air diffusion process. This implies that the diffusion coefficients for dry air and water vapor cannot be independent and the relation between both coefficients is given by:

$$\pi_{da}^* = \frac{M_{da}}{M_v} \pi_v^* \quad (18)$$

Then the dry air mass flow rate can be expressed as:

$$\vec{g}_{da} = -\frac{M_{da}}{M_v} \pi_v^* \vec{\nabla} \frac{p_{da}}{p_t} - \frac{\rho_{da}}{\rho_t} K_t \vec{\nabla} p_t \quad (19)$$

175 As this flow rate is zero, a relation can be established between the molecular ratio and total pressure gradients:

$$\vec{\nabla} \frac{p_v}{p_t} = \frac{\rho_{da} M_v}{\rho_t M_{da} \pi_v^*} \vec{\nabla} p_t \quad (20)$$

Then, replacing the molecular ratio gradient in equation (15) by this expression, the following expression of the water vapor mass flow rate can be obtained:

$$\vec{g}_v = -\left(\frac{\rho_{da} M_v}{\rho_t M_{da}} + \frac{\rho_v}{\rho_t}\right) K_t \vec{\nabla} p_t \quad (21)$$

180 This expression demonstrates that in the configuration of the cup test method, if the gradient of the total gas pressure were zero, then the vapor mass flow rate would be null as well.

3.5. Diffusion vapor flow vs advection vapor flow

A first consequence of the non-uniformity of total gas pressure is that the measured vapor flow cannot be considered as a purely diffusive flow. Part of
185 this flow is obviously due to advection. From the preceding equations, it is possible to obtain an estimation of the magnitude of these two contributions to the measured overall vapor flow.

Indeed, diffusive and advective vapor mass flow rates can be written as:

$$\vec{g}_{v,diff} = -\pi_v^* \vec{\nabla} \frac{p_v}{p_t} \quad (22)$$

$$\vec{g}_{v,adv} = -\frac{\rho_v}{\rho_t} K_t \vec{\nabla} p_t \quad (23)$$

190 Using relation (20) in (22) leads to an expression of the diffusive vapor mass flow rate in which all diffusive characteristics (molecular ratio gradient, diffusion coefficient) disappear:

$$\vec{g}_{v,diff} = -\left(\frac{\rho_{da} M_v}{\rho_t M_{da}}\right) K_t \vec{\nabla} p_t \quad (24)$$

Using the perfect gas law and the definition of the molar mass of the gas mixture in (23) and (24) leads to the following equations:

$$\vec{g}_{v,diff} = -\left(\frac{(p_t - p_v) M_v}{p_t M_t}\right) K_t \vec{\nabla} p_t = -(1 - c_v) \frac{M_v}{M_t} K_t \vec{\nabla} p_t \quad (25)$$

$$\vec{g}_{v,adv} = -\left(\frac{p_v M_v}{p_t M_t}\right) K_t \vec{\nabla} p_t = -c_v \frac{M_v}{M_t} K_t \vec{\nabla} p_t \quad (26)$$

195 Then, the contribution of each vapor transfer phenomenon clearly appears, and we can write:

$$\vec{g}_{v,diff} = (1 - c_v) \vec{g}_v \quad (27)$$

$$\vec{g}_{v,adv} = c_v \vec{g}_v \quad (28)$$

At atmospheric pressure and for moderate temperatures (which can be considered as normal building conditions), the order of magnitude of c_v is 10^{-2} . Thus, it can be assumed that under such conditions, most of the vapor flow
200 that is measured by the cup test method is due to diffusion. But at higher temperatures and/or under lower gas pressures, this basic assumption fails and the measured vapor flow cannot be considered as purely diffusive.

3.6. Impact of the total pressure non-uniformity on the estimated value of the water vapor diffusion coefficient

In order to estimate the measurement error that inevitably appears when the gas pressure non-uniformity is not taken into account, it is necessary to look

back at the equations. From equation (19), considering that the dry air mass flow rate in steady-state is zero, it is possible to write a relation between the gradient of gas pressure and the gradient of water vapor partial pressure :

$$\vec{\nabla} p_t = \frac{1}{c_v + (1 - c_v)A} \vec{\nabla} p_v \quad (29)$$

Where:

$$A = \frac{M_v K_t}{M_t \pi} \quad (30)$$

and :

$$\pi = \frac{\pi_v^*}{p_t} \quad (31)$$

205 A is a non-dimensional number that roughly represents the ratio between the gas advective permeability and the water vapor diffusive permeability.

Thanks to this expression, it is possible to write the total water vapor mass flow rate across the sample as:

$$\vec{g}_v = -\frac{\pi_v^*}{p_t} \left(1 + \frac{c_v(A-1)}{c_v + (1-c_v)A}\right) \vec{\nabla} p_v \quad (32)$$

210 This last expression can be compared to the expression of the same mass flow rate as it is written when the gas pressure non-uniformity is not taken into account:

$$\vec{g}_v = -\frac{\pi_{app}^*}{p_t} \vec{\nabla} p_v \quad (33)$$

Where π_{app}^* is the apparent diffusion coefficient of water vapor.

The relative measurement error can then be estimated by writing the equality
215 of both expressions of the vapor mass flow rate:

$$\frac{\pi_{app}^* - \pi_v^*}{\pi_v^*} = \frac{c_v(A-1)}{c_v + (1-c_v)A} \quad (34)$$

As mentioned above, at atmospheric pressure and for a moderate temperature, the order of magnitude of c_v is 10^{-2} . Assuming that, it is possible to get a

graphical representation of the measurement relative error as a function of the non-dimensional number A .

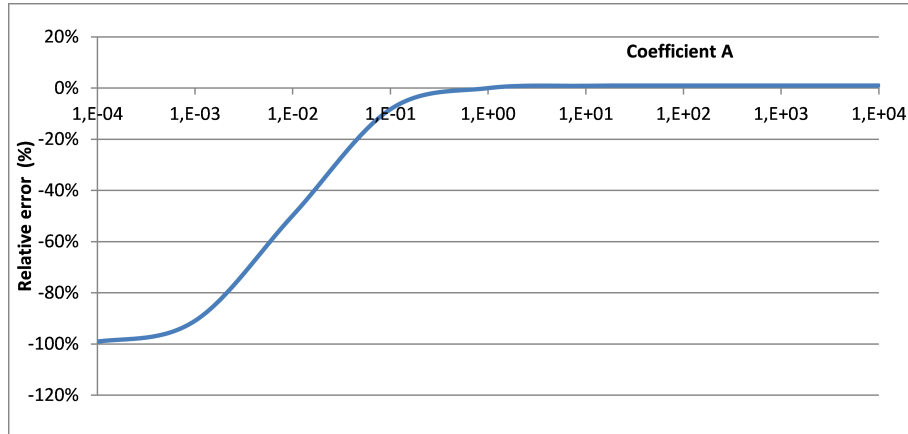


Figure 5: Representation of the relative error measurement as a function of the non-dimensional number A

220 For values of A above 1, the water vapor diffusion coefficient can be slightly overestimated. This situation is due to the addition of the advective part of the vapor flow to the diffusive one in materials with high gas permeability and/or low vapor permeability. For measurements at atmospheric pressure, this error remains very weak. But for smaller A values (e.g., materials with low advective

225 gas permeability and/or high diffusive water vapor permeability), the underestimation of the diffusion coefficient can be tremendous. This is because the total gas pressure adaptation in the cup leads to a lower difference of c_v between the two faces of the sample, which results in a lower diffusive vapor flow.

For a given material, if a value of its advective gas permeability is known, it is

230 possible to calculate the coefficient A after a water vapor permeability measurement by the cup test method. Then, it can be concluded whether the measured permeability is underestimated or not. However, if an underestimation occurs, it is impossible to estimate the true water vapor permeability. The calculated value of A is based on an underestimated water vapor permeability value. Thus,

235 the real permeability value must be higher and the corresponding A value must
 be lower which results in a greater underestimation. This demonstrates that the
 potential correction procedure is a diverging process which makes it impossible
 to determine the real water vapor permeability of low A -value material.

240 *3.7. Validity of the cup test method for the measurement of the water vapor
 permeability*

Using the non-dimensional number A in the expression of the dry air mass
 flow rate (equation (14)) results in the equation:

$$\vec{g}_{da} = -\frac{\pi_{da}^*}{p_t} (\vec{\nabla} p_{da} - \frac{p_{da}}{p_t} (1 - A) \vec{\nabla} p_t) \quad (35)$$

245 For materials with a very low A value (lower than 10^{-2}), A can be neglected
 in this expression which then results in:

$$\vec{g}_{da} = -\pi_{da}^* \vec{\nabla} \frac{p_{da}}{p_t} \quad (36)$$

This expression shows that for such materials, the dry air mass flow is purely
 diffusive. It is established that the dry air mass flow rate is zero during the
 steady state of a cup test. This means that for materials with a very low
 A value, the diffusive dry air mass flow rate is zero. As a consequence, the
 250 diffusive vapor mass flow rate is zero as well and the cup test method cannot
 be used to estimate the water vapor permeability of a material for which the A
 value is considerably smaller than 1.

4. Experimental

In order to get a first experimental check of this theoretical assumption of
 255 total pressure non-uniformity, Pr. Wahbi JOMAA (Bordeaux University) had
 tested a circular sample of oak, 27mm thick with a 90mm diameter, in the
 frame of the ADEME research project MACHA [25]. The vapor flow across
 the sample was perpendicular to the main orientation of the wood fibers. The

testing conditions were 50% RH in the climatic room and 11% RH in the cup
260 for a 60 °C temperature. During the test, a small-sized wire-free differential
manometer was introduced in the cup to monitor the total gas pressure differ-
ence between both sides of the sample.

In steady state, a vapor mass flow rate of $1.9210^{-7} kg/(m^2.s)$ was measured
265 across the sample. The following figure shows the evolution of the total gas
pressure difference between both sides of the wood during the test.

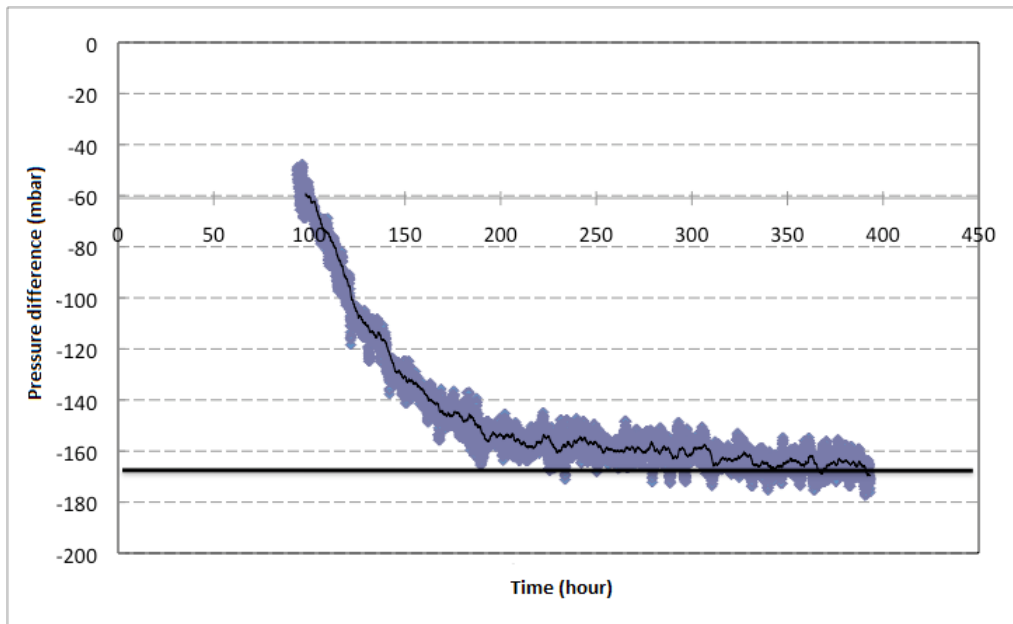


Figure 6: Gas pressure difference between both sides of the wood sample during a cup test

When the steady state was reached, the gas pressure in the cup had de-
creased by more than 160 *mbar* (16000 *Pa*). To our knowledge, this is the first
270 experimental evidence of the gas pressure non-uniformity during a cup test. Of
course, this single exploratory test cannot be considered as definitive proof of
the validity of this new vision of the cup test method. The same experiment will

have to be reproduced in various conditions and with various materials in order to estimate the relevance of this theoretical approach. Nevertheless, the measured pressure difference seems large enough to reject *a priori* the hypothesis of experimental bias.

5. Results and Discussion

5.1. Simulation of the exploratory test on oak:

The experimental test presented in chapter 5 (cup test method for a sample of oak with measurement of the gas pressure difference) has been simulated with the SYRTHES tool.

The simulated conditions (same as the conditions of the test):

- HR in the cup: 11% ;
- HR in the climatic chamber: 50%;
- Temperature: 60°C;

The initial conditions used of the oak sample for this simulation in SYRTHES are:

- Temperature: 60°C;
- Water vapor pressure: 5000Pa;
- External total gas pressure: 101325Pa;

The boundary conditions used for this simulation in SYRTHES are:

- Total gas pressure: 101325Pa;
- Exchange coefficients for water vapor flow on the surface air/salt solution:
 $h_{pv} = 5.46e^{-3}Kg.m^{-2}.s^{-1}$ and $h_{pt} = 1.29e^{-7}Kg.m^{-2}.s^{-1}.Pa^{-1}$;
- Exchange coefficients for dry air flow on the surface air/salt solution:
 $h_{da} = 0Kg.m^{-2}.s^{-1}$ and $h_{pt} = 0Kg.m^{-2}.s^{-1}.Pa^{-1}$;

- Exchange coefficients for water vapor flow on the surface climatic chamber/material: $h_{pv} = 5.46e^{-3}Kg.m^{-2}.s^{-1}$ and $h_{pt} = 1.29e^{-7}Kg.m^{-2}.s^{-1}.Pa^{-1}$;
- Exchange coefficients for dry air flow on the surface climatic chamber/material:
300 $h_{pv} = 5.46e^{-3}Kg.m^{-2}.s^{-1}$ and $h_{pt} = 1.29e^{-7}Kg.m^{-2}.s^{-1}.Pa^{-1}$;
- Exchange coefficients for heat: $h_c = 10W/m^2.K$;

The exchange coefficients for water vapor and total gas pressures are calculated using Lewis relation:

$$h_{pt} = \frac{h_c M_t}{\rho_{air} T R C_p}$$

$$h_{pv} = \frac{h_c M_v P_t}{\rho_{air} T R C_p}$$

with: M_v : Water vapor molar mass(kg/mol), M_t : air molar mass (kg/mol),
305 ρ_{air} : air density (Kg/m^3), R : The ideal gas constant, T ; Temperature (K), C_p : Specific heat of air ($J/Kg.K$).

The characteristics of oak used in the SYRTHES simulation 5.1 were calculated using the experimental results of the cup test and the identification method of the model parameters proposed in chapter 4 hereafter. The identification led to
310 the characteristics presented in Table 5.1.

Characteristics	$K (m^2)$	$\pi_v^* (kg/m.s)$	$\pi_{da}^* (kg/m.s)$
Adopted values	1.07×10^{-17}	6.768×10^{-8}	10.5×10^{-7}

Table 1: Main transfer characteristics of oak used for simulations

Figure 7 shows the calculated difference of total gas pressure in the simulated cup test method. The value of the pressure differential in the steady state is $159.5mbar$. We notice that the simulated evolutions of total gas pressure are different between the experimental results and simulation. But since, we don't
315 know the real initial conditions of the test, and one can suspect that they can be responsible of this different dynamic behavior.

In order to explore this impact, figure 8 shows the impact of the initial conditions on the simulations. We can see that the results of the steady-state are the same, but the simulations dynamics change with initial conditions.

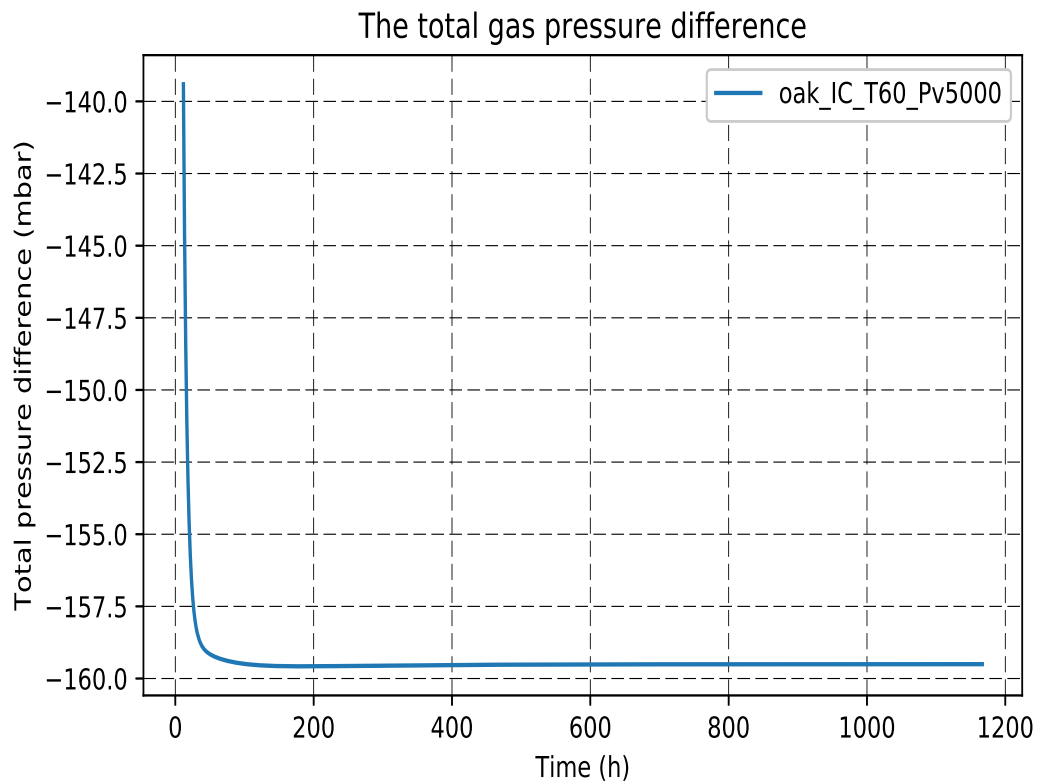


Figure 7: Simulation of Gas pressure difference between both sides of the wood sample during a cup test

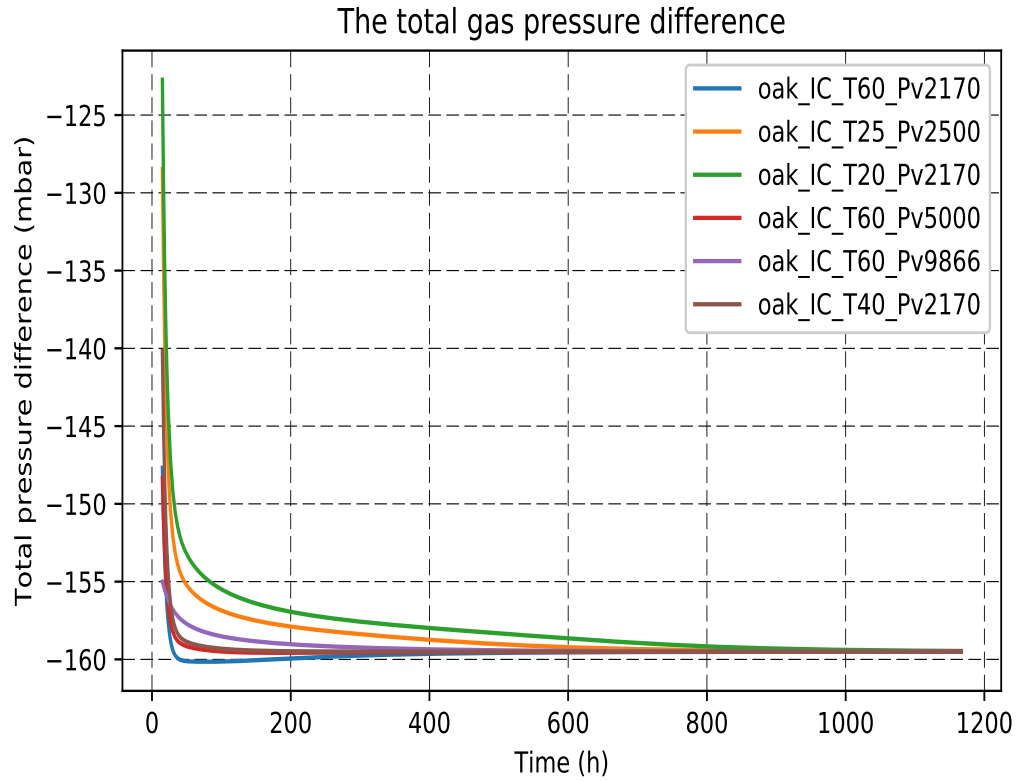


Figure 8: Simulation of Gas pressure difference between both sides of the wood sample for different initial conditions

We also, calculated the water vapor flow rate using SYRTHES. At the steady state, we find $1.91 \times 10^{-7} Kg/(m^2.s)$ for a sample of $27mm$ thick (figure 9). The difference between the experimental flow rate in the steady-state ($1.92 \times 10^{-7} Kg/(m^2.s)$) and the one simulated is negligible.

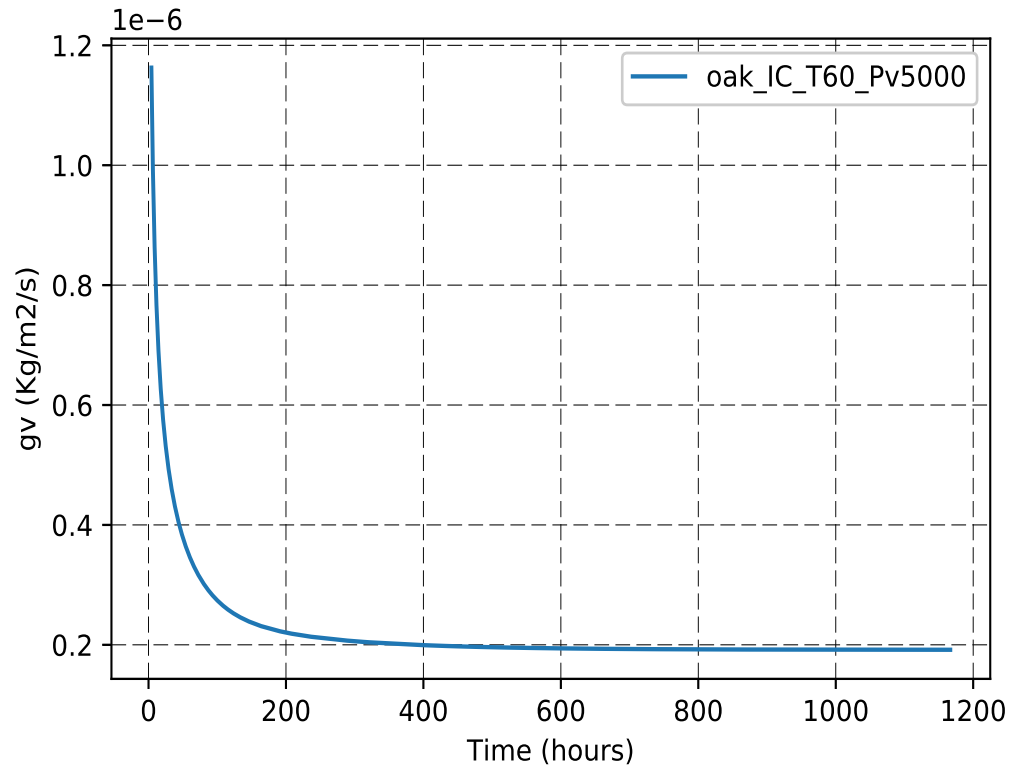


Figure 9: Simulation of water vapor mass flow rate

325 In this part of the article, it has been shown that it is possible to find
reasonable material characteristics for which all the experimental statements
(vapor mass flow rate, partial pressure, and total pressure differences) can be
reproduced by modeling. Of course, this is neither proof of the model validity
nor indicative of the measurement quality. But it is nevertheless a marker of
330 consistency of the proposed approach and an incentive to go further in the
analysis of the cup test method as an indicator of hidden properties of tested
materials.

5.2. Analysis of the influence of the diffusion coefficient and of the gas permeability:

335 The cup test method can be analysed through numerical simulation using a 2 layers 1D isothermal configuration with specific boundary conditions as described in Figure 10.

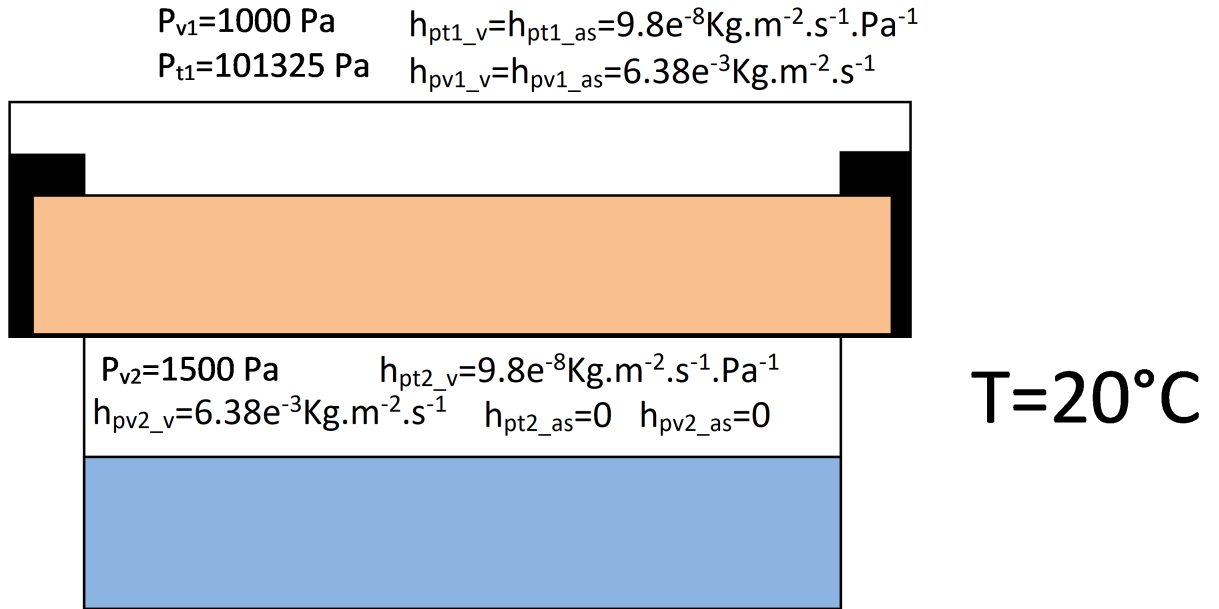


Figure 10: 1D configuration and boundary conditions for cup test method simulations

Simulations have been carried out with SYRTHES [17].

340 The 2 cm thick tested sample has been given the basic mass transfer characteristics which are generally expected for ordinary concrete and are as given in table 5.2. This material is a cementitious material with basic characteristics chosen to approach the behavior of ordinary concrete.

Characteristics	K_t (kg/m.s.Pa)	π_v^* (kg/m.s)	π_{da}^* (kg/m.s)
Adopted values	6.5×10^{-12}	8.5×10^{-7}	10.5×10^{-7}

Table 2: Main transfer characteristics of material used for simulations

The cup test method is supposed to be able to estimate the water vapor diffusion coefficient π_v^* through the measurement of the vapor mass flow rate
345 when the steady state has been reached.

Figure 11 shows the simulated vapor mass flow rate evolutions for five different values of the vapor diffusion coefficient. For these simulations the reference vapor diffusion coefficient $\pi_v^* = 8.5 \times 10^{-7} \text{ kg/m.s}$ (Case Piv) has been divided
350 (Cases Piv.10-1 and Piv.10-2) or multiplied (Cases Piv.10+1 and Piv.10+2) by a factor 10 or 100 while all other parameters are kept at their initial values given in Table 5.2.

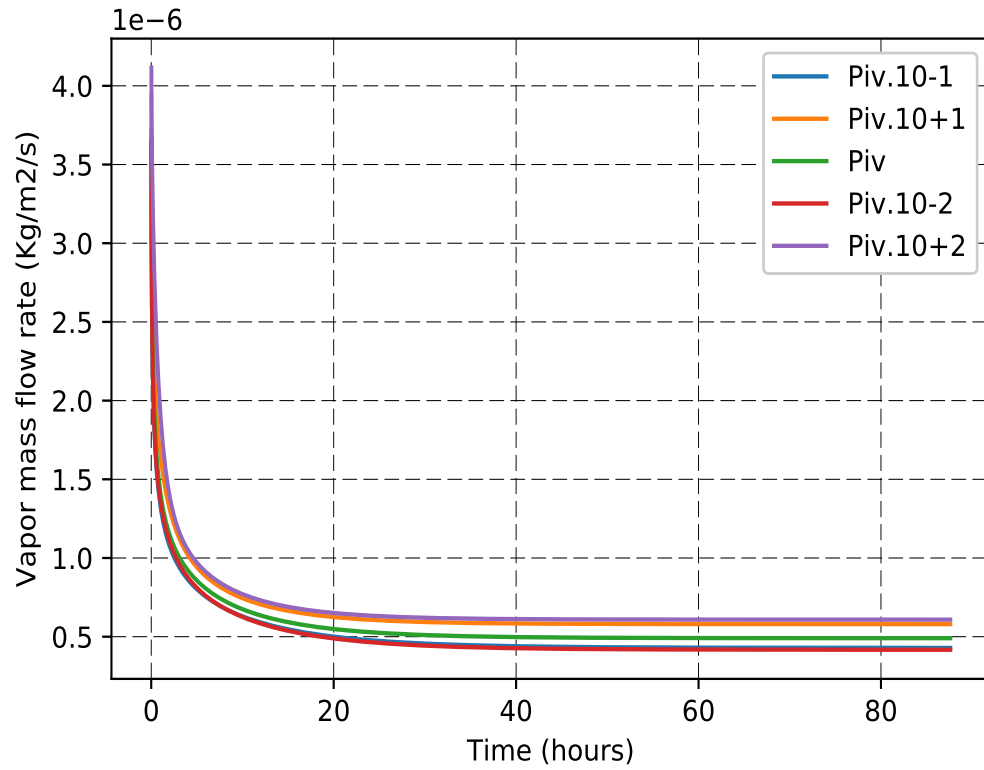


Figure 11: Evolution of the simulated vapor mass flow rate for five values of the vapor diffusion coefficient

It appears clearly that for such a material with a rather low gas permeability (K_t), the vapor mass flow rate in steady state is almost the same for all values of the vapor diffusion coefficient. Obviously, this criterion cant be considered as a satisfactory indicator of the vapor diffusion coefficient.

The next figure shows the evolution of the simulated vapor mass flow rate for five different values of the gas permeability (K_t) while all other parameters are set at their initial values.

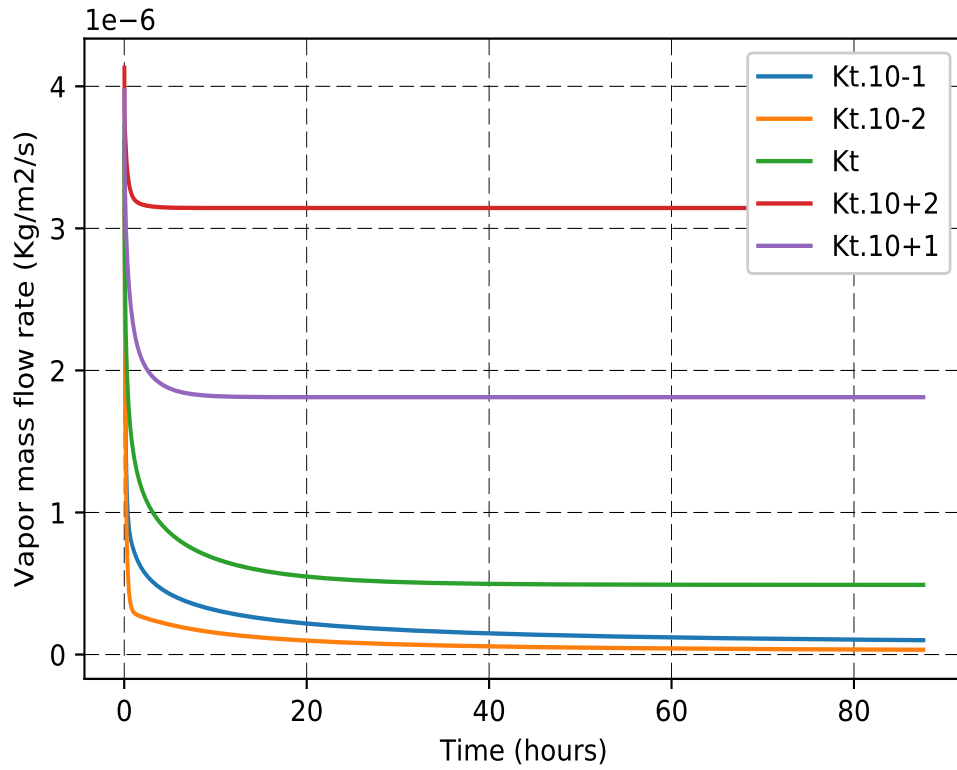


Figure 12: Evolution of the simulated vapor mass flow rate for five values of the gas permeability

These simulation results show that the vapor mass flow rate is in these cases much more influenced by the gas permeability than by the water vapor diffusion coefficient.

365

This can be explained through the evolution of the gas pressure difference between the both sides of the sample for the previous simulation conditions.

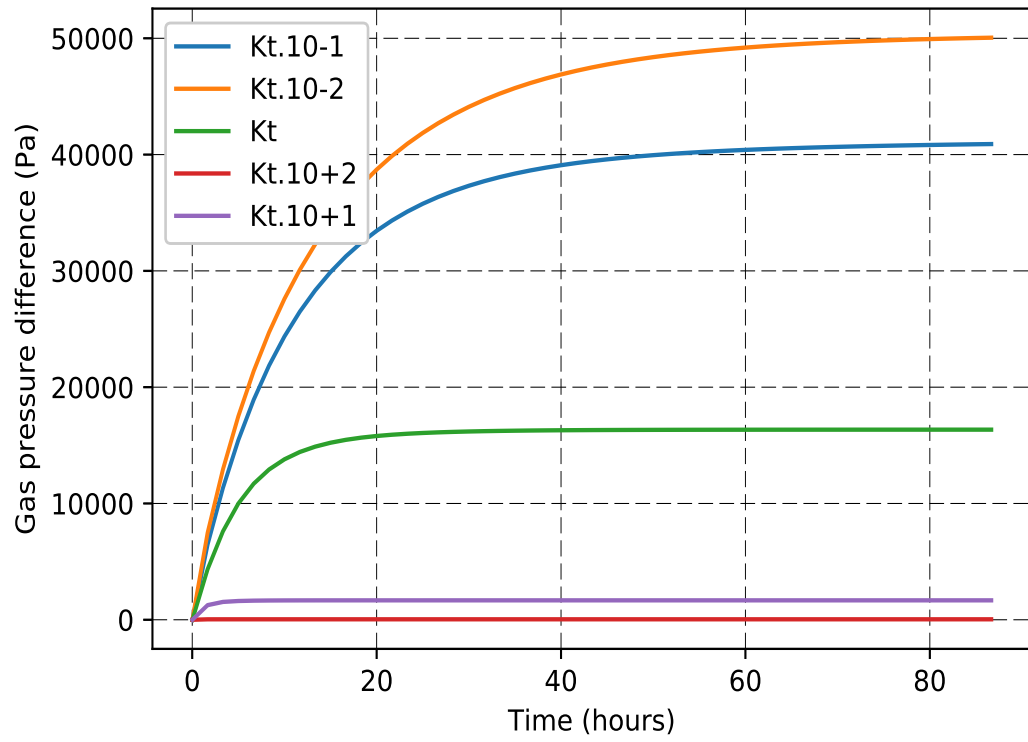


Figure 13: Gas pressure difference between the both sides of the sample for five values of the gas permeability

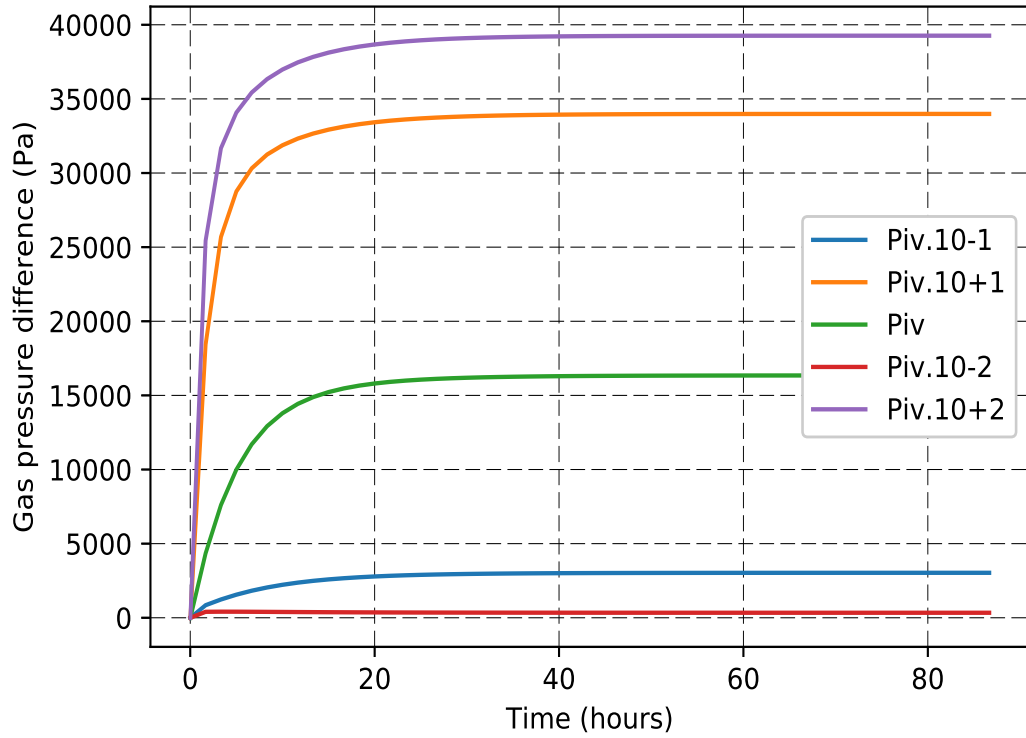


Figure 14: Gas pressure difference between the both sides of the sample for five values of the vapor diffusion coefficient

370 A lower gas permeability involves a higher gas pressure difference between the two faces of the tested sample. The higher gas pressure is located on the side of the higher vapor pressure, i.e. into the cup for the simulation conditions. Thanks to the simulation results, it is possible to calculate the water vapor molecular ratio on each side of the sample for the five previous gas permeability values.

375

	Kt.10+2	Kt.10+1	Kt	Kt.10-1	Kt.10-2
In the cup	14.2×10^{-3}	14.2×10^{-3}	12.7×10^{-3}	10.6×10^{-3}	10.0×10^{-3}
Out of the cup	10.3×10^{-3}	10.1×10^{-3}	9.9×10^{-3}	9.8×10^{-3}	9.8×10^{-3}
Difference	3.9×10^{-3}	4.1×10^{-3}	2.7×10^{-3}	0.7×10^{-3}	0.1×10^{-3}

Table 3: Water vapor molecular ratios on the two sides of the simulated sample for the previous simulation configurations

It appears clearly that the driving force of the vapor diffusion (the difference of water vapor molecular ratio) becomes smaller and smaller when the gas permeability is decreasing. This means that the measured vapor flow, which can be considered as purely diffusive in these conditions, is significantly affected by
380 the gas permeability which is not a characteristic of diffusion.

Given these simulation results, it can then be considered that the measurement of the water vapor diffusion coefficient should take into account this gas pressure effect which is mainly due to the very specific testing conditions and
385 to the advective characteristics of the tested material.

5.3. Proposal of a new test procedure and a new goal for the cup test method

As it has been shown in the previous part, the cup test method can be inefficient and even not applicable for the determination of the water vapor permeability of materials with very low A values and low hygroscopic behavior. For
390 other materials, this method can be used, but the measurement can result in an important underestimation of the water vapor permeability. This is mainly due to the impact of the total gas pressure evolution in the cup which is neither controlled nor measured. Thus, the real difference of the molecular ratio between the two faces of the sample is unknown and the actual diffusive water
395 vapor permeability cannot be determined.

We now propose modifying the usual cup test procedure to overcome this difficulty. The modification consists of measuring the total gas pressure in the

climatic room and the cup during the test. In this way, the water vapor partial pressure, the total gas pressure, and the water vapor molar ratio can be
 400 estimated on both sides of the sample. This alternative approach can offer the opportunity to measure simultaneously the advective gas permeability K_t and the diffusion coefficient π_v^* .

Taking into account the perfect gas law, the expression (21) can be transformed
 405 into:

$$\vec{g}_v = -\frac{M_v}{\bar{M}_t} K_t \vec{\nabla} p_t \quad (37)$$

In steady state and for a 1D configuration, the scalar writing of this expression gives:

$$K_t = \frac{\bar{M}_t g_v e}{M_v \Delta p_t} \quad (38)$$

Where e is the thickness of the sample and \bar{M}_t is the average value of the molar mass of the gas in the sample which can be expressed as a function of the average water vapor molar fraction:

$$\bar{M}_t = (1 - \bar{c}_v) M_{as} + \bar{c}_v M_v \quad (39)$$

This leads to a measurable expression of the advective gas permeability:

$$K_t = \frac{[(1 - \bar{c}_v) M_{as} + \bar{c}_v M_v] g_v e}{M_v \Delta p_t} \quad (40)$$

From equation (27), a relation between total and diffusive water vapor mass
 410 flow rate can be obtained:

$$-\pi_v^* \vec{\nabla} \frac{p_v}{p_t} = (1 - c_v) \vec{g}_v \quad (41)$$

Which results in a scalar expression that can be transformed to get a measurable value of the diffusive vapor transfer coefficient:

$$\pi_v^* = \frac{g_v e}{\Delta c_v} (1 - \bar{c}_v) \quad (42)$$

Where \bar{c}_v is the average value of the vapor molar fraction which can be estimated from their values measured on both sides of the sample: $\bar{c}_v = \frac{c_{v1} + c_{v2}}{2}$.

415 Of course, this new methodology remains theoretical. Its validity and efficiency
still need to be appreciated through real measurements in actual test conditions.

This method can also be considered as an indirect measurement method for
the gas phase relative permeability in non-saturated conditions, which has been
420 up to now a very challenging operation. Indeed, this parameter can be calculated
from K_t provided an accurate value of the intrinsic permeability of the material.

6. Conclusions

This paper highlights, with the help of some experimental and simulation
425 examples, the importance of the potential impact of total gas pressure on mass
transfer in building materials. This impact cannot be correctly assessed without
the use of a realistic equation representing gas diffusion mass flow rate, based
on a gradient of the gas molar fraction. It can be observed in this paper that
the experimental measurement of an important gas pressure difference between
430 both sides of a sample during a cup test is an indirect validation of this gas
diffusion expression.

The experimental modification proposes to render the cup test method more
efficient for the water vapor permeability determination, and more universal as
435 it could also be used for the estimation of advective gas permeability.

To challenge this experimental method, a complete test program integrated
into a national research project in France SmartRéno [26], is set up. In this
program, this new method will be tested on different materials, in different ex-
440 perimental conditions by several laboratories. First results are expected by the
middle of 2021.

In this paper, we focused on vapor transport in dry materials at a macro-

scopic scale in the cup test method. The liquid transport and its impact on the
445 apparent water vapor permeability were outside the scope of our study. Never-
theless, it would be interesting to study unsaturated materials with important
surrounding relative humidity. In such conditions, both liquid and vapor phases
of water are influencing the measured vapor flows. Certainly, the influence of
gas pressure should then be revisited regarding new phenomena including evap-
450 oration and condensation areas at the frontiers of liquid water islands acting as
water vapor short-circuit.

More specifically, one can hope and expect that this new perception of a
very old and universally practised test method will create a positive reaction of
455 curiosity in the many labs that are used to carrying out these experiments. We
sincerely hope this paper can contribute to the launching and the development
of an ambitious experimental program that would turn the old-fashioned cup
test method into a very recent and innovative experimental activity.

460 **References**

- [1] H. Glaser, Graphisches Verfahren zur Untersuchung von Diffusionsvorgänge., Vol. 10, Kalfetechnik, 1959, pp. 345–349.
- [2] J. R. Philip, D. A. De Vries, Moisture movement in porous materials under temperature gradients, *Eos, Transactions American Geophysical Union* 38 (2) (1957) 222–232. doi:<https://doi.org/10.1029/TR038i002p00222>.
465
- [3] A. Luikov, Heat and mass transfer in capillary-porous bodies, Vol. 1 of *Advances in Heat Transfer*, Elsevier, 1964, pp. 123–184. doi:[https://doi.org/10.1016/S0065-2717\(08\)70098-4](https://doi.org/10.1016/S0065-2717(08)70098-4).
- 470 [4] C. Rode, P. Hansen, K. Hansen, Combined heat and moisture transfer

in building constructions, Ph.D. thesis, Technical University of Denmark, Lyngby (September 1990).

- [5] P. Crausse, Etude fondamentale des transferts couplés de chaleur et d'humidité en milieu poreux non saturé, Ph.D. thesis, Institut National Polytechnique de Toulouse, Toulouse, France (1983).
475
- [6] A. Karagiozis, Wufi-ornl/ibp hygrothermal model, 2001.
- [7] Wufi, <https://wufi.de/>.
- [8] Delphin, <http://bauklimatik-dresden.de/delphin/documentation.php>.
- [9] TRNSYS, A transient systems simulation program,
480 <https://sel.me.wisc.edu/trnsys/> (2017).
- [10] EnergyPlus, Energyplus, <https://energyplus.net/>.
- [11] M. Mainguy, Modèles de diffusion non linéaire en milieux poreux. applications à la dissolution et au séchage des matériaux cimentaires, Ph.D. thesis, Ecole Nationale des Ponts et Chaussées, France (1999).
- [12] V. Baroghel-Bouny, M. Mainguy, O. Coussy, Isothermal drying process in
485 weakly permeable cementitious materials - assessment of water permeability, 1999, pp. 59–80.
- [13] M. Mainguy, O. Coussy, V. Baroghel-Bouny, Role of air pressure in drying of weakly permeable materials, Journal of Engineering Mechanics 127 (2001) 582–592. doi:doi:10.1061/(ASCE)0733-9399(2001)127:6(582).
490
- [14] Iso 12572 :2016, hygrothermal performance of building materials and products – determination of water vapour transmission properties – cup method.
- [15] A. Miquel, Détermination expérimentale des caractéristiques hydriques des matériaux du bâtiment : contribution à la mise au point et validation de
495 techniques nouvelles, Ph.D. thesis (1997).

- [16] A. Tveit, Measurements of moisture sorption and moisture permeability of porous materials, no. 45, Oslo, Norway, 1966.
- [17] Syrthes, //rd.edf.com/syrthes.
- [18] T. Duforestel, Des transferts couplés de masse et de chaleur à la conception bioclimatique: près de 30 ans de recherches sur l'efficacité énergétique des bâtiments., Mémoire d'habilitation à diriger les recherches, Université Claude Bernard Lyon I (2015), pp. 23–47.
- [19] J. Virgone, Vers une méthode de conception hygro-thermique des batiments performants hygro-bat (2014).
- [20] M. Woloszyn, N. Pierrès, Y. Kedowidé, J. Virgone, A. Trabelsi, Z. Slimani, E. Mougel, R. Reymond, H. Rafidiarison, P. Perre, F. Pierre, R. Belarbi, I. Nabil, K. Abahri, T. Bejat, A. Piot, E. Wurtz, T. Duforestel, M. Colmet Daâge, O. Legrand, Vers une méthode de conception hygro-thermique des batiments performants: démarche du projet hygro-bat, Conference IBPSA France, Arras, France, 2014.
- [21] P. Rousset, P. Perré, P. Girard, Modification of mass transfer properties in poplar wood (*p. robusta*) by a thermal treatment at high temperature, *Holz als Roh- und Werkstoff* 62 (2004) 113–119. doi:10.1007/s00107-003-0459-5.
- [22] A. Tarmian, R. Remond, H. Dashti, P. Perré, Moisture diffusion coefficient of reaction woods : Compression wood of *picea abies* l. and tension wood of *fagus sylvatica* l. 46 (2012) 405–417. doi:https://doi.org/10.1007/s00226-011-0413-3.
- [23] O. Vololonirina, M. Coutand, B. Perrin, Characterization of hygrothermal properties of wood-based products impact of moisture content and temperature, *Construction and Building Materials* 63 (2014) 223–233. doi:https://doi.org/10.1016/j.conbuildmat.2014.04.014.

- [24] S. Zohoun, E. Agoua, G. Degan, P. Perré, An experimental correction proposed for an accurate determination of mass diffusivity of wood in steady regime, *Heat and Mass Transfer* 39 (2003) 147–155. doi:10.1007/s00231-002-0324-9.
- [25] MACHA, Définir l'impact des transferts de masse sur les transferts de chaleur (2010).
- [26] SmartRéno, Le projet smart réno (fiabiliser, professionnaliser, valoriser la rénovation énergétique) du programme du ministère de la transition écologique et solidaire sur le dispositif des certificats économies d'énergie, <https://smart-reno.recherche.univ-lr.fr/>.